A Triple Band Polarization Insensitive Ultrathin Metamaterial Absorber for S- C- and X-Bands

Amit K. Singh[*], Mahesh P. Abegaonkar, and Shiban K. Koul

Abstract—In this paper, design of a triple band ultrathin compact polarization insensitive metamaterial absorber for S-, C- and X-band applications is proposed. The proposed absorber consists of periodic arrangement of a modified triple circular slot ring resonator as unit cell printed on the top of a continuous metal backed FR-4 dielectric substrate. The proposed absorber is ultrathin having thickness of $\lambda_0/135.66$ at the lowest absorption center frequency. The measured wide stable absorption bands of 0.40 GHz, 0.45 GHz and 0.47 GHz with absorption peaks of 97%, 96.45% and 98.20% at absorption center frequencies of 2.90 GHz, 4.18 GHz and 9.25 GHz respectively are observed. The temperature profile of absorber is measured by using lock in infrared thermography, and a temperature increase of 1°C at absorbing frequency as compared to non-absorbing frequency is observed. The absorber is demonstrated to be polarization insensitive to TE and TM polarized angles of incidence of electromagnetic wave with wide angular stability up to 45°. The absorber is fabricated and tested in an anechoic chamber. Experimental results agree well with measured ones.

1. INTRODUCTION

Microwave absorbers are artificially engineered materials for absorbing electromagnetic wave to reduce EMI EMC and for stealth applications. Design of traditional absorber is complex. Metamaterials are great solution for this. Metamaterial is an array of sub-wavelength fundamental unit cells having controlled material properties such as permeability and permittivity. Metamaterials are used widely for various antenna applications like to enhance radiation characteristic of antenna, for beam forming and beam steering. Metamaterial absorbers have attracted great attention due to their wide range applications and easy fabrication characteristic.

A perfect metamaterial absorber was reported by Landy et al. [1] using a metallic structure. Polarization insensitive wide-band metamaterial absorber by using resistive loading and multi-layer structure sub wavelength unit cell is designed in [2, 3]. Active metamaterial wide-band wide-angle absorber is designed and reported in [4]. An ultrathin wearable absorber is designed by using compact metamaterial unit cell in [5]. Multi-band polarization insensitive absorbers are designed in [6–8]. A compact ultrathin multi-band absorber is designed by using fractal broken cross with Jerusalem cross loading in [9, 18], and multi-band absorbers using compact unit cells are designed in [10–14]. These absorbers are not ultrathin and compact with multi-band operation at the same time.

In this paper, the design of a triple band ultrathin polarization insensitive metamaterial absorber for S- C- and X-bands is proposed. The same absorber can be further extended with more absorption bands. A compact modified triple circular slot ring resonator (MTCsRR) is used as fundamental unit cell to design the absorber. An array of MTCsRR unit cells is fabricated on top of a metal backed FR-4 substrate. The absorption phenomenon is verified by measuring reflection from the fabricated absorber in an anechoic chamber. The TE and TM polarization insensitive characteristic with oblique angle of incidence of EM wave is also measured. The temperature profile of absorber is measured by using lock in infrared thermography, and it was found to increase surface temperature at absorption frequencies.

* Corresponding author: Amit Kumar Singh (amitkumarcareiitd@gmail.com).
The authors are with the Centre for Applied Research in Electronics, Indian Institute of Technology, Delhi 110016, India.

2. DESIGN OF UNIT CELL

In this section, design of unit cells for absorber design is discussed. The proposed metamaterial absorber is made up of a modified triple circular slot ring resonator as unit cell. A triple circular ring resonator is proposed first. The perimeter of rings is selected as half of the wavelength at optimum resonant frequency. The rings are further miniaturized by using capacitive loading. Capacitive loads are created by designing metallic radial slots on the ring. Radial slots are introduced on the metallic ring to reduce the resonance frequency. It is observed that compactness of 22.50% is achieved due to outer modified circular ring resonator (MCRR) to have absorption centre frequency at 2.9 GHz as compared to the conventional circular ring resonator. The additional radial slot on the MCRR increases equivalent capacitance of MCRR, resulting in decrease in resonant frequency [15, 17]. The proposed MTCsRR unit cell geometry with detailed dimension is shown in Fig. 1(a). The MTCsRR unit cell is simulated using CST microwave studio with perfect electric boundary along Y axis, perfect magnetic boundary along X axis and a waveguide port along Z axis as shown in Fig. 1(b).
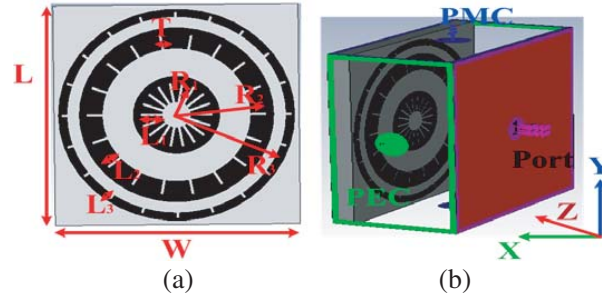

Figure 1. (a) Geometry of proposed MTCsRR unit cell and (b) boundary condition to simulate MTCsRR unit cell. The Dimensions are $R_1 = 2.00$, $R_2 = 5.00$, $R_3 = 6.50$, $L_1 = 1.45$, $L_2 = 1.10$, $L_3 = 0.40$, $T = 0.20$, $L = 14.00$ and $W = 14.00$ (all dimensions are in mm).

The absorptivity of proposed unit cell structure under normal incidence of electromagnetic waves is given as $A = 1 - |S_{11}|^2 - |S_{21}|^2$. The transmission coefficient $|S_{21}|^2$ of the proposed structure will be zero due to metal backing. Hence absorptivity is given by $A = 1 - |S_{11}|^2$. The simulated reflection coefficient and absorptivity are shown in Fig. 2(a) and Fig. 2(b), respectively. A simulated triple band resonance with centre frequencies of 2.90 GHz, 4.20 GHz and 9.30 GHz with -10 dB reflection bandwidths of 0.27 GHz, 0.24 GHz and 0.28 GHz respectively indicating more than 90% absorption is obtained. The equivalent circuit model of MTCsRR unit cell is designed and plotted in Fig. 3. The inductances L_1, L_2 and L_3 are due to inductive metallic section of CRRs, and capacitances C_1, C_2 and C_3 are due to capacitive slot on CRRs. The equivalent circuit parameters like equivalent inductance and
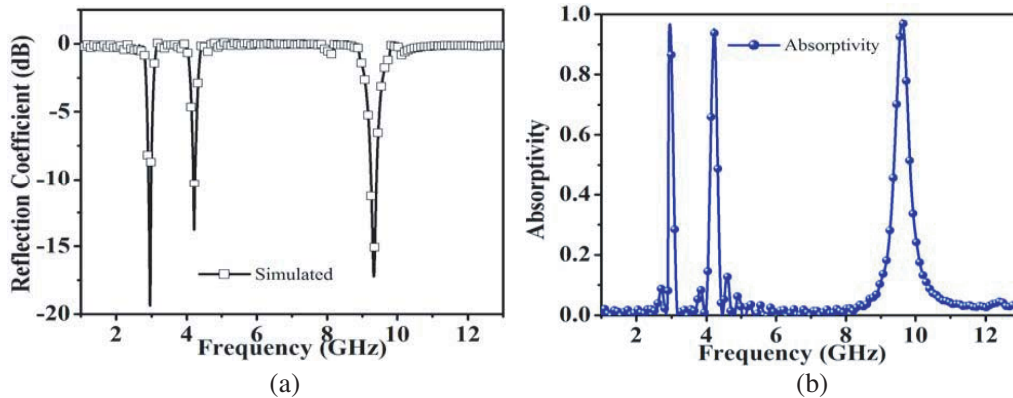

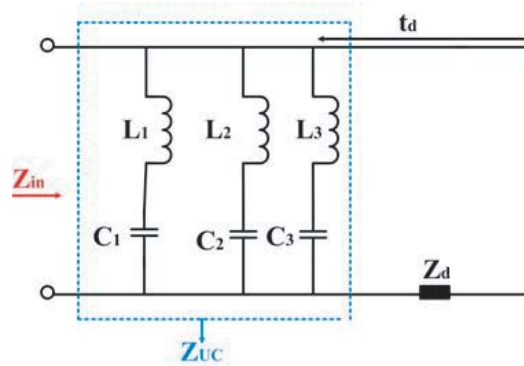**Figure 2.** (a) Simulated reflection coefficient and (b) simulated absorptivity.

Figure 3. The equivalent circuit model of MTCsRR unit cell.

capacitance due to all CRRs are also calculated by using [6, 7]. In the equivalent circuit, "Z_{UC}" is the total equivalent impedance due to MTCsRR unit cell, and "Z_d" is the impedance of dielectric substrate of thickness t_d. The total input impedance "Z_{in}" is due to parallel combination of "Z_{UC}" and "Z_d". The circuit simulated reflection coefficient using ADS software and EM simulated reflection coefficient using CST microwave studio are compared and found matching with small error. The dielectric with optimized unit cell dimensions is used to provide impedance matching.

To validate the cause of resonance at these frequencies, the simulated H-field and E-field distributions on MTCsRR are studied and plotted in Fig. 4 and Fig. 5, respectively. The normally incident plane wave (along Z Axis) having E-field along X axis induces capacitive effect and H-field along Y axis induces inductive effect resulting in resonance at some particular resonant frequency. The maximum concentration of E- and H-fields at first resonant frequency of 2.9 GHz is found on outer MCRR, at the second resonant frequency of 4.2 GHz on middle MCRR and at the third resonant frequency of 9.2 GHz on inner MCRR. The circulating H-field induces different surface currents on the MTCsRR at different frequencies. The surface current distributions at all three resonant frequencies are plotted in Fig. 6. It is observed that the surface currents on MTCsRR and the ground plane at resonant frequencies are anti-parallel to each other forming a loop, resulting in absorption of respective
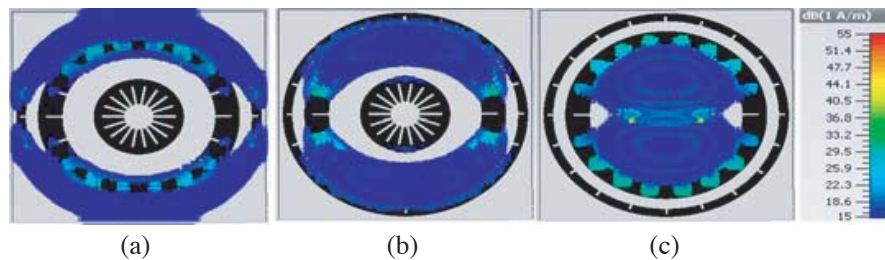

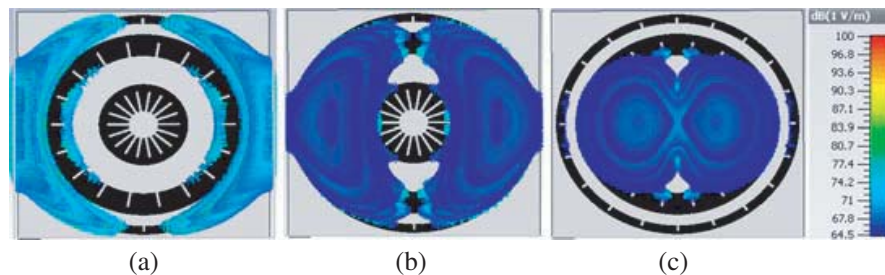**Figure 4.** Simulated H-field distribution, (a) 2.9 GHz, (b) 4.2 GHz and (c) 9.2 GHz.

Figure 5. Simulated E-field distribution, (a) 2.9 GHz, (b) 4.2 GHz and (c) 9.2 GHz.
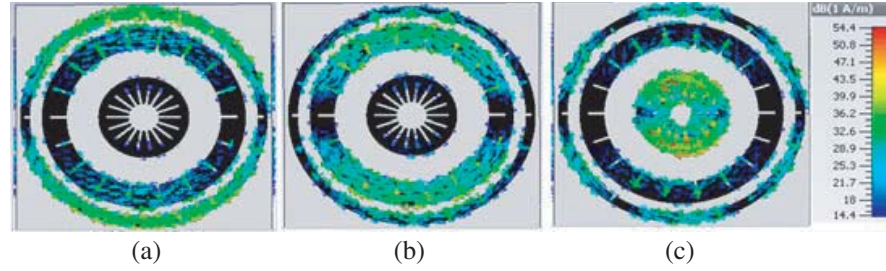
Figure 6. Simulated surface current distribution, (a) 2.9 GHz, (b) 4.2 GHz and (c) 9.2 GHz.

frequencies.

The E-field, H-field and surface current distributions predict that the first resonant band is generated due to outer MCRR, second resonant band generated due to middle MCRR, and third resonant band generated due to inner MCRR. The change in dimensions of MCRR will change the respective resonant frequency. The mean radius of outer MCRR "R_1", middle MCRR "R_2" and inner MCRR "R_3" is varied, and the corresponding changes in reflection coefficients are plotted in Fig. 7(a), Fig. 7(b) and Fig. 7(c), respectively. It is observed that increasing the mean radius of MCRR increases the ring perimeter that causes increase in effective inductance and capacitance resulting in decrease in resonant frequency. Similarly, decreasing the mean radius of MCRR increases its resonant frequency.

The capacitive slots on the metallic ring acts as a capacitive load due to in plane E-field incidence on MCRR. The effect of dimensional change of slot is studied and plotted in Fig. 7(d). It is observed that the change in slot dimensions changes all the resonant frequencies predicting that all resonant frequencies depend on slot dimensions. Hence all the resonant frequencies can also be controlled by using capacitive lode tuning. It is also observed by the parametric variations shown in Fig. 7 that all the three absorption bands can be controlled independently.
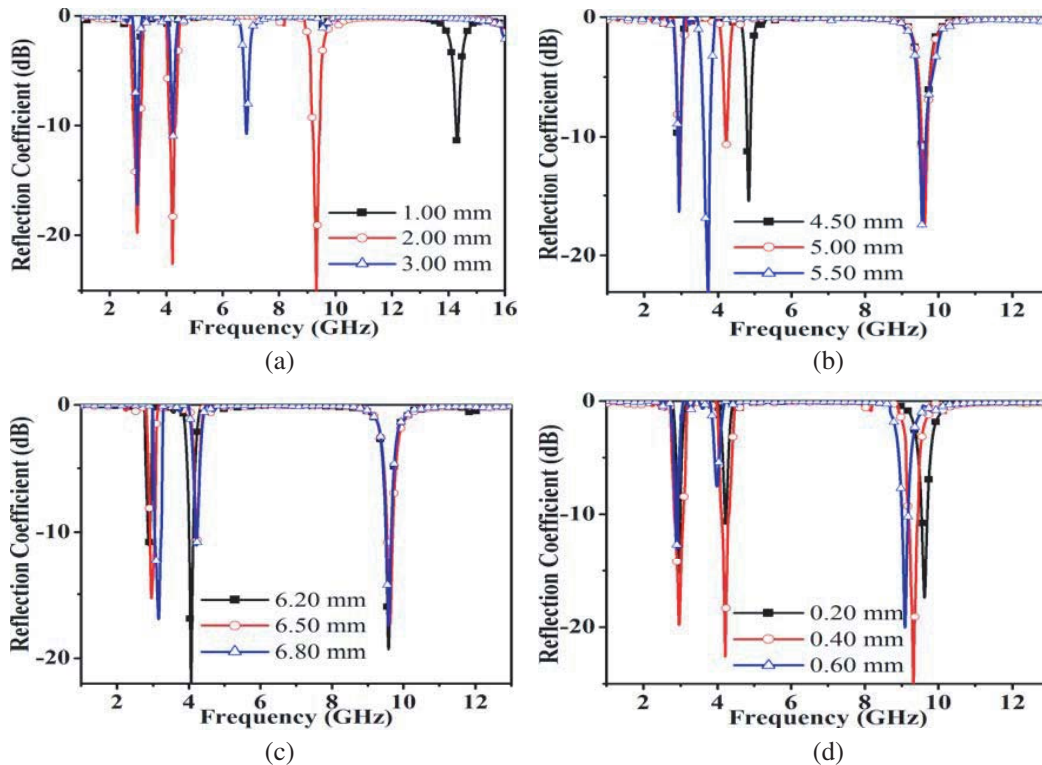

Figure 7. Simulated reflection coefficient with variation in mean radius of (a) inner ring resonator "R_1", (b) middle ring resonator "R_2", (c) outer ring resonator "R_3" and (d) variation in slot thickness.

3. EXPERIMENTAL RESULTS

In this section, fabrication of prototype absorber and measurement results are discussed. A 12×12 array of MTCsRR unit cells is designed and printed. The prototype of ultrathin triple band metamaterial absorber is fabricated using photolithography on an FR-4 substrate having permittivity of 4.3, dielectric thickness of 0.762 mm, and copper thickness of 0.035 mm. The fabricated prototype of metamaterial absorber is shown in Fig. 8(a). The absorption response of absorber is measured in an anechoic chamber. Two standard gain wide-band double ridge horn antennas separated by foam pyramidal absorber are placed inside the anechoic chamber. One of the ridge horn antennas acts as a transmitter and the other one as a receiver. The measurement setup is shown in Fig. 8(b). The back ground noise of anechoic chamber is measured first. The back ground noise is observed to be less than -60 dB. To measure the absorptivity/reflection characteristic of fabricated absorber, a metal plate of same dimension as fabricated absorber is placed in the far field of the measurement setup, and reflection characteristic is recorded first. Next, the metal plate is replaced by fabricated absorber, and reflection characteristic is measured. The actual reflection due to proposed absorber surface is different between the two reflection characteristics. The measured back ground noise, reflection due to metal plate and reflection due to proposed absorber are plotted in Fig. 9.
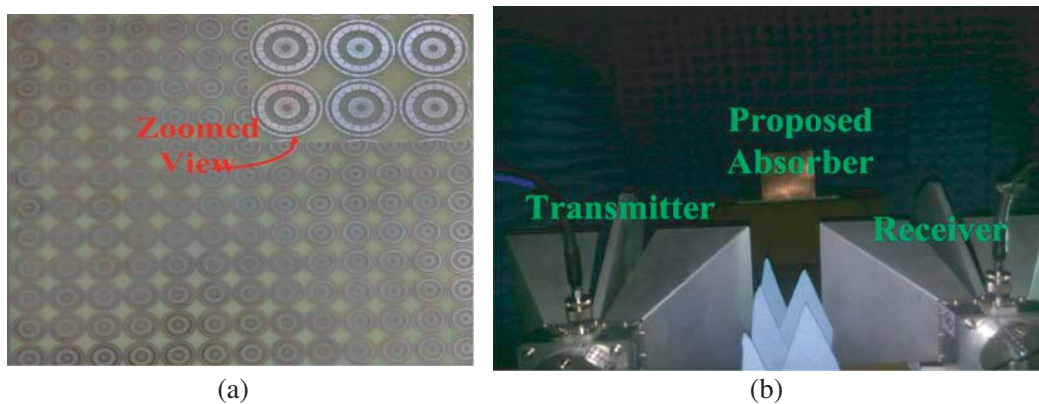

(a)　　　　　　　　　　　　　　(b)

Figure 8. (a) Fabricated prototype absorber and (b) the used free space measurement setup for characterizing the fabricated absorber.
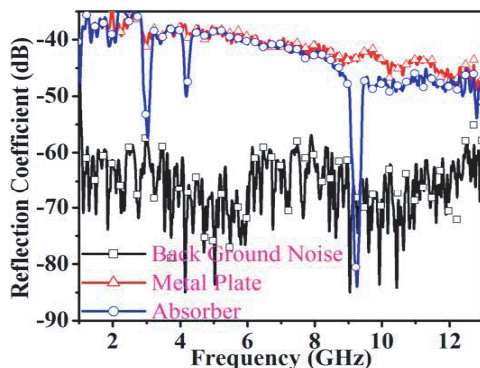

Figure 9. The measured reflection coefficients. (Back ground noise, reflection due to metal plate and reflection due to absorber).
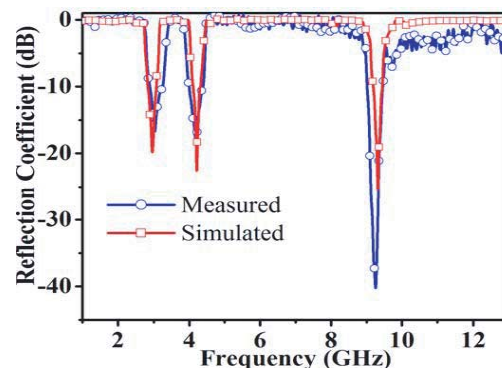
Figure 10. Measured and simulated reflection coefficient due to absorber.

The simulated and measured reflection characteristics of the proposed absorber are plotted in Fig. 10, which shows a good agreement. Measured -10 dB reflection band of 0.40 GHz at first absorption frequency of 2.9 GHz, 0.45 GHz at second absorption frequency of 4.18 GHz, and 0.47 GHz at third
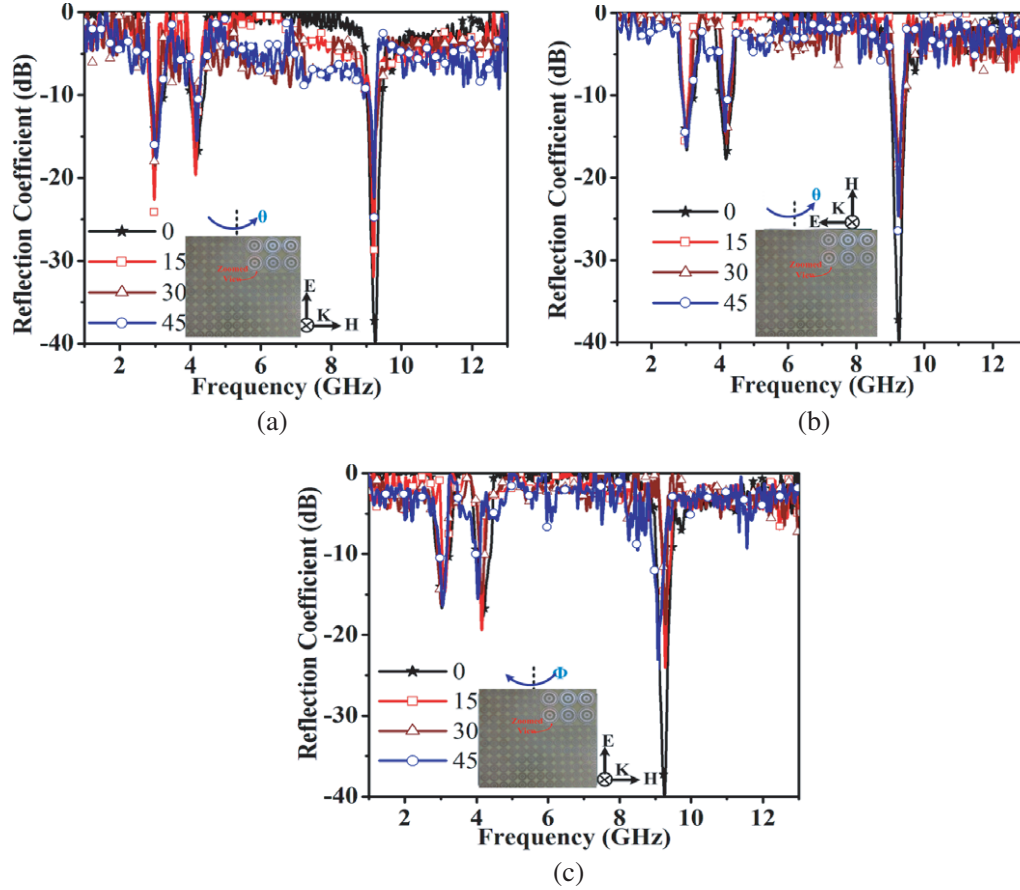
(a)

(b)

(c)

Figure 11. The measured reflection coefficient (absorptivity) due to various angle of incidence of (a) TE polarized EM wave, (b) TM polarized EM wave and (c) oblique incidence of EM wave.

absorption frequency of 9.25 GHz predicting more than 90% absorption are obtained.

To verify the performance of the polarization insensitive absorber, absorptivity characteristic of prototype absorber due to various angles of incidence of TE and TM polarized EM waves are studied. The angle between the two double ridge horn antennas is changed in its TE and TM planes to generate EM wave with various angles of incidence of TE and TM polarized EM waves. The reflection characteristics of prototype absorber due to various angles of incidence of TE and TM polarized EM waves are measured and plotted in Fig. 11(a) and Fig. 11(b), respectively. It is observed that the proposed absorber is insensitive to various angles of incidence of TE and TM polarized EM waves with wide angular stability up to 45°. The advantage of multi-band absorber as compared to broad band absorber is to avoid unwanted interference with required information signal in the ultra-wideband region.

The absorber is studied for various oblique angles of incidence of EM wave in elevation plane. The measured reflection characteristics due to various oblique angles of incidence of EM wave are plotted in Fig. 11(c). It is observed that the absorber is insensitive to various oblique angles of incidence of EM wave up to 45°.

The absorption of EM wave by absorber causes increase in surface temperature of the absorber. The surface temperature change of absorber is studied by using lock in infrared (IR) thermography as reported in [16, 17]. The measurement setup is shown in Fig. 16. The absorber surface is excited by a wide-band double ridge horn acting as a radiator having power level of 10 dBm. The temperature profile is measured by thermal images of absorber as recorded by IR camera. First, the temperature profile at non-absorbing frequency of 6.0 GHz is recorded (Fig. 12(a)). Next, the temperature profiles at absorbing frequencies of 2.9 GHz, 4.18 GHz and 9.25 GHz as shown in Fig. 12(b), Fig. 12(c) and
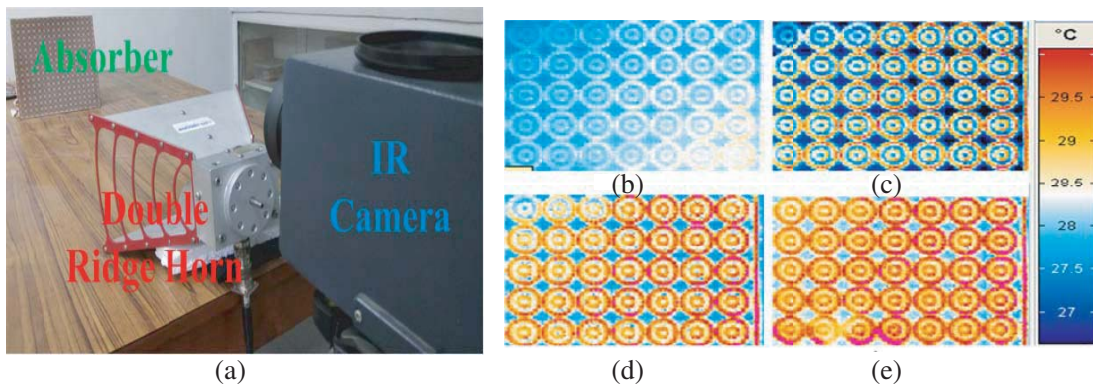
Figure 12. (a) Measurement setup for temperature profile measurement, measured temperature profile on absorber surface at (b) 6 GHz, (c) 2.9 GHz, (d) 4.18 GHz and (e) 9.25 GHz.

Fig. 12(d) are recorded. A temperature increase of 1°C at absorbing frequencies as compared to non-absorbing frequency is observed.

The proposed absorber is compared with several similar absorbers reported earlier in Table 1 in terms of "λ_0", where "λ_0" is the wavelength at list resonant absorption frequency. As observed, the proposed absorber is found to be more ultrathin and compact with wide multi-band absorption characteristics.

Table 1. Comparison of proposed absorber with several reported absorbers.

Ref.	Unit Cell Dimension (λ_0)	Thickness (λ_0)	Absorption Frequency (GHz)
7	$0.124\lambda_0$	$\lambda_0/92.24$	3.2, 9.45, 10.90
8	$0.207\lambda_0$	$\lambda_0/30.125$	6.22, 8.76, 13.05
9	$0.204\ \lambda_0$	$\lambda_0/125$	1.5, 4.3, 6.3
10	$0.167\ \lambda_0$	$\lambda_0/90$	4.19, 9.34, 11.48
Proposed Absorber	**$0.135\lambda_0$**	**$\lambda_0/135.66$**	**2.9, 4.2, 9.60**

4. CONCLUSION

A triple band polarization insensitive compact ultrathin metamaterial absorber for S- C- and X-band applications is successfully demonstrated. The absorber is designed by using capacitive slot loading, and compactness of 22.50% as compared to conventional absorber is achieved. The thickness of the proposed absorber is $\lambda_0/135.66$, where λ_0 is the free space wavelength at the first centre frequency of absorption (2.9 GHz) making the absorber ultrathin. The wide absorption bandwidths of 0.40 GHz, 0.45 GHz and 0.47 GHz with more than 90% absorption at absorption center frequencies 2.90 GHz, 4.18 GHz and 9.25 GHz having absorption peak of 97%, 96.45% and 98.20% respectively are observed. The proposed absorber is polarization insensitive with wide angular stability up to 45° in azimuth and elevation plane. The proposed absorber is found insensitive to TE and TM polarized various angles of incidence of EM wave with wide angular stability up to 45°. The temperature profile of absorber is measured using IR thermography. The absorption of EM wave by absorber results in increase in surface temperature by 1°C. The absorber prototype can be used for EMI/EMC reduction, and it can be easily extended for more band applications.

REFERENCES

1. Landy, I., S. S. Sajuyigbe, J. J. Mock, D. R. Smith, and W. J. Padilla, "A perfect metamaterial absorber," *Phys. Rev. Letters*, Vol. 100, 207402, 2008.

2. Lin, X. Q., P. Mei, P. C. Zhang, Z. Z. D. Chen, and Y. Fan, "Development of a resistor-loaded ultrawideband absorber with antenna reciprocity," *IEEE Transactions on Antennas and Propagation*, Vol. 64, No. 11, 4910–4913, Nov. 2016.

3. Yoo, M., H. K. Kim, and S. Lim, "Angular- and polarization-insensitive metamaterial absorber using subwavelength unit cell in multilayer technology," *IEEE Antennas and Wireless Propagation Letters*, Vol. 15, 414–417, 2016.

4. Fan, Y., et al., "An active wideband and wide-angle electromagnetic absorber at microwave frequencies," *IEEE Antennas and Wireless Propagation Letters*, Vol. 15, 1913–1916, 2016.

5. Tak, J. and J. Choi, "A wearable metamaterial microwave absorber," *IEEE Antennas and Wireless Propagation Letters*, Vol. 16, 784–787, 2017.

6. Chaurasiya, D., S. Ghosh, S. Bhattacharyya, A. Bhattacharya, and K. V. Srivastava, "Compact multi-band polarisation-insensitive metamaterial absorber," *IET Microwaves, Antennas & Propagation*, Vol. 10, No. 1, 94–101, Jan. 9, 2016.

7. Zhai, H., C. Zhan, Z. Li, and C. Liang, "A triple-band ultrathin metamaterial absorber with wide-angle and polarization stability," *IEEE Antennas and Wireless Propagation Letters*, Vol. 14, 241–244, 2015.

8. Hasan, M. M., M. R. I. Faruque, and M. T. Islam, "A tri-band microwave perfect metamaterial absorber," *Microw. Opt. Technol. Lett.*, Vol. 59, 2302–2307, 2017.

9. Heydari, S., P. Jahangiri, A. Sharifi, F. B. Zarrabi, and S. Arezomand, "Fractal brokencross with Jerusalem load absorber for multiband application with polarization independence," *Microw. Opt. Technol. Lett.*, Vol. 59, 1942–1947, 2017.

10. Mishra, N., D. Choudhary, R. Chowdhury, K. Kumari, and R. Chaudhary, "An investigation on compact ultra-thin triple band polarization independent metamaterial absorber for microwave frequency applications," *IEEE Access*, Vol. 5, No. 99, 4370–4376, 2017.

11. Zheng, D., Y. Cheng, D. Cheng, Y. Nie, and R. Z. Gong, "Four-band polarization-insensitive metamaterial absorber based on flower-shaped structures," *Progress In Electromagnetics Research*, Vol. 142, 221–229, 2013.

12. Dincer, F., M. Karaaslan, E. Unal, K. Delihacioglu, and C. Sabah, "Design of polarization and incident angle insensitive dual-band metamaterial absorber based on isotropic resonators," *Progress In Electromagnetics Research*, Vol. 144, 123–132, 2014.

13. Wang, G.-D., J.-F. Chen, X. Hu, Z.-Q. Chen, and M. Liu, "Polarization-insensitive triple-band microwave metamaterial absorber based on rotated square rings," *Progress In Electromagnetics Research*, Vol. 145, 175–183, 2014.

14. Singh, A. K., M. P. Abegaonkar, and S. K. Koul, "Penta band polarization insensitive metamaterial absorber for EMI/EMC reduction and defense applications," *2017 IEEE MTT-S International Microwave and RF Conference (IMaRC)*, 1–5, Ahmedabad, 2017.

15. Singh, A. K., M. P. Abegaonkar, and S. K. Koul, "High gain and high aperture efficiency cavity resonator antenna using metamaterial superstrate," *IEEE Antennas and Wireless Propagation Letters*, Vol. 16, 2388–2391, 2017.

16. Muzaffar, K., S. Tuli, and S. Koul, "Determination of polarization of microwave signals by lock-in infrared thermography," *IETE Journal of Research*, Vol. 62, No. 1, 81–90, 2016.

17. Singh, A. K., M. P. Abegaonkar, and S. K. Koul, "Dual- and triple-band polarization insensitive ultrathin conformal metamaterial absorbers with wide angular stability," *IEEE Transactions on Electromagnetic Compatibility*, Vol. 3, 1–9, 2018.

18. Bakır, M., M. Karaaslan, F. Dincer, K. Delihacioglu, and C. Sabah, "Tunable perfect metamaterial absorber and sensor applications," *Journal of Materials Science: Materials in Electronics*, Vol. 27, No. 11, 12091–12099, 2017.